

A NEW HYBRID MULTI-FOCUS IMAGE-FUSION USING DMWT WITH FFT TRANSFORMS

ADNAN HADI MAHDI AL-HELALI¹, JAMAL S. ZRAQOU², WISSAM.ALKHADOUR³,
ABDULLA AL-NUEMI⁴

^{1,2,3,4}Faculty of Information Technology, Isra University, Amman, Jordan

¹adnan_hadi@iu.edu.jo, ²jamal_sam@iu.edu.jo, ³Wissam.Alkhadour@iu.edu.jo, ⁴abdstn@iu.edu.jo

ABSTRACT

A new technique of image fusion combining multi-focus images is proposed. It employs Discrete Multi-Wavelet Transform (DMWT) together with Fast Fourier Transform (FFT). Two source images are decomposed by FFT and DMWT first, then, treated by three different fusion rules, namely maximum selection rule, gradient rule, and absolute maximum selection rule for merging coefficients low and high-frequency sub-bands. This technique is experimentally implemented and tested on the often-used grayscale images, then the obtained results are compared with other multi-focus techniques, such as the Simple Pixels Averaging (SPA), the Principal Component Analysis (PCA), and wavelet transform (WLT). It was found that the proposed method has outperformed the formers in terms of image fusion. The comparison included the various metrics, such as correlation (CORR), MI, EN, QE, QAB/F, SD, root mean square error (RMSE), AG, and SF. Hence, based on objective and subjective evaluations, the proposed technique is promising for fusion multi-focus images.

Keywords: DMWT, Image Processing, Image-fusion, Multi-focus, WLT, FFT.

1. INTRODUCTION

Due to the limited depth of field of optical lenses in CCD devices, it is often impossible to take an image that has all relevant objects in focus, which means that if an object is in focus in the scene, another object will be out of focus (blurred) [1].

A common idea to solve this problem is multi-focus image fusion, which combines multi images of a different focus target in the same scene into a composite image that focuses on a sharp image so that the new image is more suitable for recognition, detection, or visualization tasks [2].

The Fusion can broadly be classified as, fusion in the time domain and the frequency domain and the image-fusion methods vary in technical complexity, starting with the simplest pixel averaging technique which is the simplest up to the most sophisticated and accurate techniques, such as the multi-resolution and complex techniques that implement artificial intelligence concepts. These techniques are Multi-Focus, Multi-Sensor, Multi-Modality, and Multispectral image fusions.

The image-fusion technique was employed in many vital applications, such as national security checkpoints, military, law enforcement, computer

vision, medical diagnosis imaging, manufacturing, and robots [3].

Recently, many time domain and frequency domain schemes for such multi-focus were developed. These schemes have been developed and published aiming to achieve an acceptable level of multi-focus image applications. For more detailed information about available image-fusion methods, a comprehensive survey is reported by Jiang Q. et al. [4]. It includes explanations and comparisons for a list of the most important and widely used multi-focus image-fusion methods. This survey includes the following methods.

Principal component analysis (PCA), DWT, Dual tree DWT (i.e. DTDWT), nonsubsampling contourlet transforms (NSCT), subsampled shelet transforms (NSST), Laplacian pyramid (LP), Gaussian Patch (GP), stationary wavelet transforms (SWT), discrete cosine harmonic wavelet (DCHWT), Standard deviation (SD), stationary wavelet transform with fusion symmetry (SWT+FS).

Generally, the Frequency domain multi-resolution analysis that is usually employed for image-fusion processes is achieved by one of the available transforms, such as pyramid transform, discrete wavelet transforms, multiwavelet

transform, etc. However, the discrete wavelet transform (DWT) provides comparatively better spatial and spectral localization of image information. It is preferred for the multi-focus, Multi-Modality, and as well as remote sensing image-fusion [5]. Some extensions to the classical wavelet transform have been used for image fusion. The discrete multiwavelet transform-based image fusion methods are proposed in [6], [7] for multi-focus image fusion. Multi wavelet offers the advantages of combining symmetry, orthogonally, and variable support, which cannot be achieved by scalar two-channel wavelet systems at the same time. This method is suitable for hardware implementation because of its simple arithmetic operations; however, artifacts may be formed in the fused image.

In this paper, a new hybrid multi-focus image fusion using DMWT mixed with FFT Transforms is proposed and implemented. It has manifested an improved multi-focus image fusion behavior, results are compared with some previously available methods. Section 2 is dedicated to the understanding and principles of the transformation techniques used in this work, namely FFT and DMWT. The proposed method for image fusion (DMWT with FFT) using three fusion rules as outlined in section 3. Results are listed and discussed in section 4 and finally, section 5 concludes the paper.

2. THEORETICAL BACKGROUND

A. Discrete Multi-Wavelet (DMWT)

Image enhancement processes such as denoising, fusion, and compression can be implemented elegantly using the wavelets technique. Wavelets are generated by scaling functions, obviously, for a single wavelet, a single scaling function is required, while for multiwavelets applications, more than one scaling function is needed. Typically, for any wavelet function $\psi(t)$, a scaling function $\phi(t)$ is associated with it. Multiwavelets have more than one scaling and wavelet function. Normally, in vector notation, these functions are expressed as shown in equation 1. and equation 2, respectively.

$$\Phi(t) = [\phi_1(t), \phi_2(t), \dots, \phi_r(t)]^T \quad (1)$$

$$\Psi(t) = [\psi_1(t), \psi_2(t), \dots, \psi_r(t)]^T \quad (2)$$

Where r is the number of wavelets involved in the process, equation 1 represents the multi-scaling function, and equation 2 represents the scalar wavelet (or simply wavelet).

Therefore, if $r=1$, then only one wavelet ($\Psi(t)$, called a scalar wavelet) is used. However, so far only multiwavelets for $r=2$ are reported by Fann [8]. The scaling function and the wavelet function for scalar wavelets are given in equation 3 and equation 4, respectively.

$$\Phi(t) = \sqrt{2} \sum_{k=-\infty}^{\infty} H_k \Phi(2t - k) \quad (3)$$

$$\Psi(t) = \sqrt{2} \sum_{k=-\infty}^{\infty} G_k \Phi(2t - k) \quad (4)$$

Where H_k and G_k are matrix filters. Hence, for each integer k there will be i.e. there are $r \times r$ matrices, providing more degrees of freedom as compared with those provided by the traditional scalar wavelet. As multiwavelets preserve a multi-channel nature, which means different sub-band structures resulting due to the signal propagating along a multifilter bank. The effect of this different sub-band structure in the multiwavelet results in deterioration in the quantization process achieved in the case of scalar wavelet [9]. Geronimo, Hadrian, and Massopust [10] proposed the multiwavelet filter (called GHM) that offers a combination of three support features; orthogonality, symmetry, and compact. Such combination was not possible by other scalar wavelet approaches [4]. Based on equation 3 and equation 4, the scaling and wavelet functions of Geronimo et. al. multi-wavelet satisfies the following dilation equations, namely equation 5 and equation 6.

$$\begin{bmatrix} \phi_1(t) \\ \phi_2(t) \end{bmatrix} = \sqrt{2} \sum_k H_k \begin{bmatrix} \phi_1(2t - k) \\ \phi_2(2t - k) \end{bmatrix} \quad (5)$$

$$\begin{bmatrix} \psi_1(t) \\ \psi_2(t) \end{bmatrix} = \sqrt{2} \sum_k G_k \begin{bmatrix} \psi_1(2t - k) \\ \psi_2(2t - k) \end{bmatrix} \quad (6)$$

Where the H_k in equation 5, for GHM system has the four scaling matrices $H_0, H_1, H_2,$ and H_3 listed in equation 7.

$$\begin{aligned} H_0 &= \begin{bmatrix} \frac{3}{5\sqrt{2}} & \frac{4}{5} \\ -\frac{1}{20} & -\frac{3}{10\sqrt{2}} \end{bmatrix}, & H_1 &= \begin{bmatrix} \frac{3}{5\sqrt{2}} & 0 \\ \frac{9}{20} & \frac{1}{\sqrt{2}} \end{bmatrix}, \\ H_2 &= \begin{bmatrix} 0 & 0 \\ \frac{9}{20} & -\frac{3}{10\sqrt{2}} \end{bmatrix}, & H_3 &= \begin{bmatrix} 0 & 0 \\ -\frac{1}{20} & 0 \end{bmatrix} \end{aligned} \quad (7)$$

Similarly, Gk of equation 6, for GHM system has also four wavelet matrices G0, G1, G2, and G3 as shown in equation 8 [11],

$$G_0 = \begin{bmatrix} -\frac{1}{20} & -\frac{3}{10\sqrt{2}} \\ \frac{1}{10\sqrt{2}} & \frac{3}{10} \end{bmatrix}, G_1 = \begin{bmatrix} \frac{9}{20} & -\frac{1}{\sqrt{2}} \\ -\frac{9}{10\sqrt{2}} & 0 \end{bmatrix}, G_2 = \begin{bmatrix} \frac{9}{20} & -\frac{3}{10\sqrt{2}} \\ \frac{1}{9} & -\frac{3}{10} \end{bmatrix}, G_3 = \begin{bmatrix} -\frac{1}{20} & 0 \\ -\frac{1}{10\sqrt{2}} & 0 \end{bmatrix} \quad (8)$$

Single level decomposition of two-dimensional (2D) images using scalar wavelet transform produces four regions or sub-bands representing low and high-frequency contents, namely LL, LH, HL, and HH as illustrated in figure 1-a. On the other hand, the decomposition of two fused images, i.e. using multiwavelet decompositions complicates the process and produces two low-frequency sub-bands and two high-frequency sub-bands in each dimension, namely L1L1, L1L2, L2L1, etc., as illustrated in figure 1-b. The obtained situation requires different analysis and more complicated procedures to benefit from the improved information contents available in such image processing combination. The four regions in the decomposed scalar wavelet of Fig 1-a are usually obtained by filtering the image using low-pass filters and high-pass filters, e.g. the data in the sub-band LL was obtained by low pass filtering of the rows and then low pass filtering of the columns of the whole image, and LH was obtained from low pass filtering of the rows and then high pass filtering of the columns, and so on.

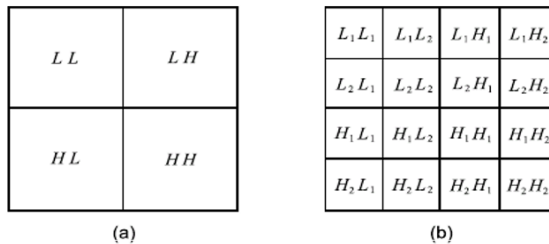


Fig 1. Image Sub-bands of Single-level Decomposition using (a) 2D-Discrete Wavelet and (b) 2D-Multiwavelets

For image-fusion multiwavelet of two images, which is the subject of consideration in this paper, two channels are used, hence two sets of coefficients are there, one for scaling and the other for the wavelet. Multiple iterations over different filters for the two images are required, hence, these

coefficients will be stored together. Similarly, the corresponding wavelet coefficients will be stored together [4].

B. Fast Fourier Transform (FFT)

FFT is the most important signal-processing tool for many years. In FFT, the signal is transformed into another domain, such as the summation of an infinite series of sines and cosines. The resulting transformation is referred to as a Fourier expansion.

The FFT algorithm is a reversible transform, i.e. if a signal represented in the time domain is transferred to an equivalent signal in the frequency domain by the FFT algorithm, it can be converted back to a time-domain signal by the inverse of this algorithm (i.e. inverse FFT). The FFT is an orthogonal transform. The forward FFT of the (NxN) image array of real numbers produces the (NxN) transformed image array of complex numbers. A forward transform is a decomposition of a certain image into its frequency components. The inverse FFT represents a re-mapping from the frequency domain to the spatial domain of an image. The Fourier domain contains, exactly, the same information as the image domain, but differently. Eq. 9 translates the signal into an FFT coefficient.

$$F(k) = \sum_{n=0}^{N-1} f(n) \exp\left(-\frac{2\pi jkn}{N}\right), \quad (9)$$

The inverse of equation 9 drives the inverse FFT given by equation 10.

$$f(k) = \frac{1}{N} \sum_{k=n}^{N-1} F(n) \exp\left(\frac{2\pi jkn}{N}\right), \quad (10)$$

Where F(k) is referred to as the Fourier coefficients of f(n), and N is the number of samples representing the signal f(n).

3. THE PROPOSED METHOD

As we know that the key point of multi-focus image fusion is to decide which portions of each image are in better focus than their respective counterparts in the associated images and then combine these regions to construct a well-focused image by certain fusion rules, which play an important role in fusion method. The basic idea of the new method is to perform DMWT and FFT on

each source image in the first step. Then, we proposed three fusion rules (maximum selection rule, gradient rule, and absolute maximum selection rule) to treat the coefficients of the low frequency and high-frequency sub-bands separately. Finally, the fused image is obtained by performing the inverse IDWT (IDMWT) and inverse of FFT (IFFT) on the combined wavelet coefficients, which were obtained by a consistency verification process from the second step. The adopted block diagram for building the new multi-focal image-fusion scheme is illustrated in Fig. 2

3.1 THE FUSION RULES

In this section, the low-pass frequency LL sub-band coefficients of input images are fused in different rules than high-pass frequency LH, HH, and HL sub-band coefficients. Three different selection rules are used for the proposed image-fusion method. These rules are described below:

Let x and y be the MWT coefficients of the two input images then the resulting of

a. Maximum fusion rule:

In this rule, the high-frequency coefficients, namely; the horizontal (rH), vertical (rV), and the diagonal (rD) are fused using the simple maximum selection as shown in the following equations 11, 12, and 13, respectively.

$$rH = \max (\detH (x) , \detH (y)) \quad (11)$$

$$rV = \max (\detV (x) , \detV (y)) \quad (12)$$

$$rD = \max (\detD (x) , \detD (y)) \quad (13)$$

Where:

\detH , \detV , and \detD are the details in the LH, HH, and HL sub-bands, respectively.

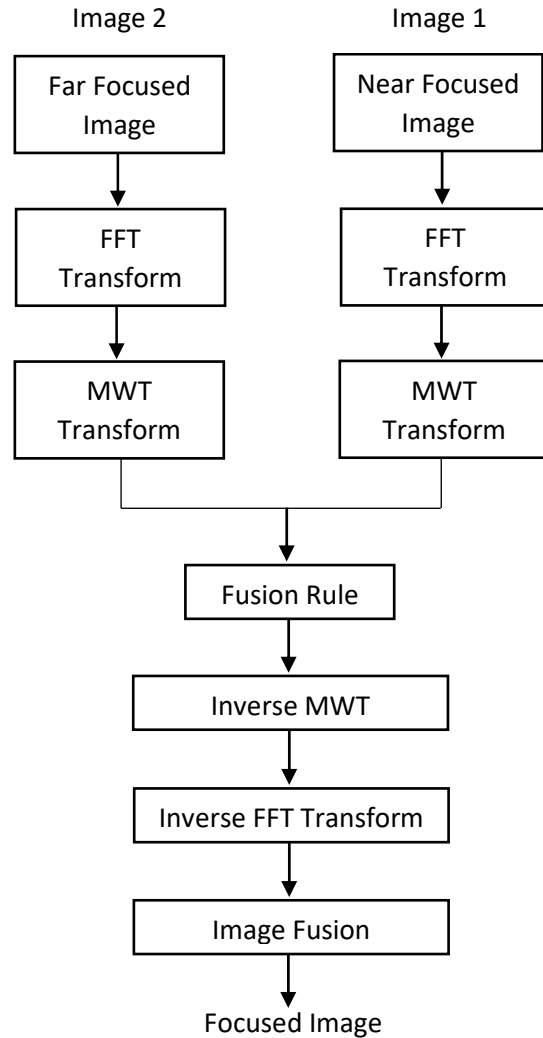


Fig. 2: A Proposed Hybrid Algorithm fusion scheme.

b. Gradient fusion rule:

Similarly, the high frequency is selected using the gradient rule as described by equations 14, 15, and 16.

$$\text{If } (g(xH) > g(yH)) \text{ then } rH = xH, \text{ else } rH = yH \quad (14)$$

$$\text{If } (g(xV) > g(yV)) \text{ then } rV = xV, \text{ else } rV = yV \quad (15)$$

$$\text{If } (g(xD) > g(yD)) \text{ then } rD = xD, \text{ else } rD = yD \quad (16)$$

Where, $g(xH)$ and $g(yH)$, $g(xV)$ and $g(yV)$, and $g(xD)$ and $g(yD)$ are the gradients of high-frequency coefficient, for input images a and b. The resulting transformation patterns, rH , rV , and rD of the LH , HH , and HL sub-bands, respectively for the fused images.

d. Absolute maximum selection:

In this fusion rule, the maximum absolute coefficients between the high-frequency coefficients of the two input images in horizontal, vertical, and diagonal directions, i.e. rH , rV , and rD , can be determined using equations 17, 18, and 19, respectively:

$$\begin{aligned} R &= (\text{abs}(xH) - \text{abs}(yH)) \Rightarrow 0, \\ rH &= R * xH + \sim R * yH \end{aligned} \quad (17)$$

$$\begin{aligned} S &= (\text{abs}(xV) - \text{abs}(yV)) \Rightarrow 0, \\ rV &= S * xV + \sim S * yV \end{aligned} \quad (18)$$

$$\begin{aligned} T &= (\text{abs}(xD) - \text{abs}(yD)) \Rightarrow 0, \\ rD &= T * xD + \sim T * yD \end{aligned} \quad (19)$$

4. RESULTS, DISCUSSION, AND COMPARISON

A. Quality Metrics

To evaluate and compare the resulting multi-focus fused images of the four different methods, various metrics were implemented. A brief definition for the metrics is given here, however, details and formulae for all metrics can be found in reference [12] by Myna and Prakash. This research is conducted based on the comprehensive overview of the existing multi-focus image fusion approaches illustrated in [13]. Relevant metrics to the measurements in this paper are:

- Root Mean Square Error (**RMSE**): It indicates the amount of change per pixel caused by processing.
- Correlation coefficient (**CORR**): It is used to measure the relevance of the fused image to input images.
- Mutual Information (**MI**): It is used to indicate the amount of information taken from the input images into the fused image.
- Edge-based on similarity ($Q^{AB/F}$): It measures the similarity between the edges transferred from the input images to the fused image.
- Standard Deviation (**SD**): It is used to give quality information of the fused image.

- Entropy (**EN**): It evaluates the information quantity in an image.
- Average Gradient (**AG**): It is used for clarity details and texture in the image.
- Spatial Frequency (**SF**): It evaluates the overall information level in different regions (activity level) of an image.
- Edge-based fusion quality index (**QE**): It is used to evaluate the object-level fusion performance objectively.

B. Real multi-focus data experiments

The proposed scheme is tested for multi-fusion on many pairs of images with various focusing arrangements. Two frequently used real multi-focus images will be included as samples to show fused images for the three selection rules under consideration. These obtained results are compared with other image-fusion methods, such as simple averaging, principle component analysis, PCA, and DWT.

The first sample of two images for Pepsi are shown in Fig. 3-a and Fig. 3-b, contain few objects at different distances from the camera. The first image focus on the Pepsi can, while in the other, the focus is on the testing card. The two images are then fused with the proposed scheme using the three selection rules described earlier. The results are shown in Fig 3-c to Fig 3-e.

From the visual observation of the resulting images, shown in Fig 13, one can be easily noticed that the texts in the resulting fused images of Fig. 3-h and Fig. 3-c to Fig. 3-e are very clear. However, they are not clear in Fig. 3-f and Fig. 3-g. These observations mean that fused images by the DWT method and the proposed (MWLT + FFT) for all the four selection rules methods have a higher contrast as compared with those fused by SPA and PCA methods.

The same pair of Pepsi images were also fused by three previously known methods namely; Simple Pixels Averaging (SPA), PCA, and DWT, then results are shown in Fig 3-f to Fig 3-h.



(a)

(b)

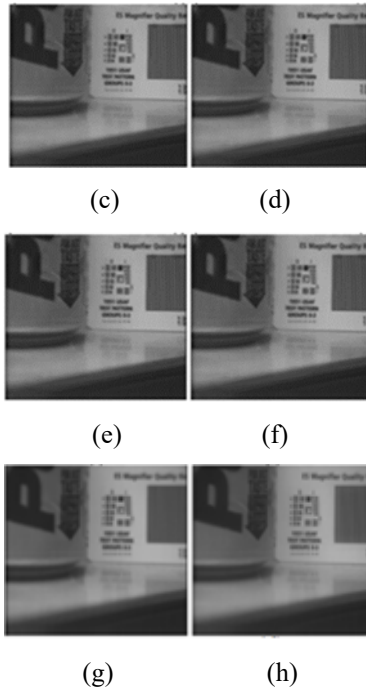


Fig. 3 Multi-focus image fusion; (a), (b) are different focus simulated (Pepsi) images; rule, (c) Maximum fusion rule, (d) gradient rule, (e) Absolute maximum rule, (f) SPA, (g) PCA, (h) DWT

Table 1: Performance comparison (for Pepsi images); (a) the proposed algorithm, (b) other fusion algorithms.

(a) The proposed algorithm			
METRIC	max. Selection	Gradient Rule	Abs. max. Selection
CORR	0.99478	0.98854	0.99493
MI	1.44772	1.44772	1.44770
EN	7.34115	7.34847	7.34144
Q _E	0.58667	0.58677	0.58685
Q ^{AB/F}	0.72210	0.72324	0.72225

(a) Other fusion algorithms			
METRIC	SPA	PCA	WALT
CORR	0.96742	0.96648	0.97923
MI	1.40661	1.44521	1.44770
EN	7.26890	7.38136	7.29180
Q _E	0.47412	0.53700	0.58620
Q ^{AB/F}	0.66840	0.57982	0.64092

C. Proposed Method Comparison

Moreover, to better evaluate the proposed image-fusion scheme, quantitative assessments are performed to evaluate five of the defined criteria, namely CORR, MI, EN, Q_{AB/F}, and Q_E. For comparison purposes, these criteria are calculated for the three selection rules methods of the proposed scheme as well as for the traditional

fusion methods; SPA, PCA, and DWT, and listed in Table 1. Observation of this table indicates that the proposed hybrid technique has better fusion performance compared with any of the other methods.

The second sample of simulated images is depicted in Fig. 4-a and Fig. 4-b, which shows images of two clocks with a different focus. Similar image-fusion experiments are performed by the proposed scheme for the three selection rules described earlier and the results are shown in Fig. 4-c to Fig. 4-e. moreover, experiments are repeated on the same two images using the three previously known methods; SPA, PCA, and DWT, where their resulted corresponding fused images are shown in Fig. 4-f to 4-h.

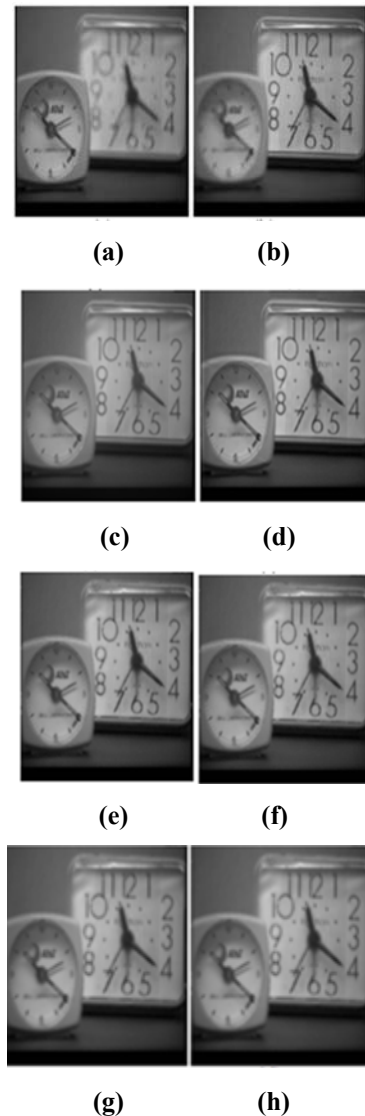


Fig. 4 Multi-focus image fusion; (a), (b) are different focus simulated (Clock) images; (c) Maximum fusion

rule, (d) gradient rule, (e) Absolute maximum rule, (f) SPA, (g) PCA, (h) DWT

By subjective evaluation, it is observed that both, the fused images for DWT method and the proposed hybrid method (MWLT+FFY) gives better fusion than those obtained by SPA, and PCA methods. Also, for the clock image example, the experiments are carried out the quantitative assessments to calculate four criteria mentioned in section 4.A (i.e. SD, RMSE, AG, and SF). These calculations were for the four selection rules using the proposed scheme as well as for the SPA, PCA, and DWT methods. The results obtained are summarized in Table 2.

Table 2: Performance comparison (for Clock images); (a) the proposed algorithm, (b) other fusion algorithms

(a) The proposed algorithm			
METRIC	Max. Selection	Gradient Rule	Abs. max. Selection
SD	78.2241	78.2235	78.2242
RMSE	6.32210	6.32325	6.32129
AG	5.71230	5.71002	5.69810
SF	8.87250	8.87220	8.87200

(b) Other fusion algorithms			
METRIC	SPA	PCA	WLT
SD	43.6230	44.0058	44.0847
RMSE	9.44310	9.32584	8.64265
AG	5.17110	5.06320	5.18220
SF	6.28411	6.28100	8.18350

Table 2 shows that the new technique offers the best performance comparing with the other three methods in terms of SD, RMSE, AG, and SF values.

The achieved real data experiments on the sample images listed in this research leads to the conclusion that all the quantitative evaluations were essentially in full agreement with corresponding visual observations. Hence, we can confidently state that the proposed hybrid image-fusion scheme that implements a successive treatment by using the DMWT and FFT based on the selection rules methods produces better-fused images than the other competitive methods.

5. CONCLUSIONS

In this paper, a simple yet effective DMWT with FFT based algorithm for multi-focus image fusion is presented. The main contribution of this work is

that we have set novel fusion rules for selecting the coefficients in the DMWT with FFT domain followed by a consistency verification process. In this method, the fusion scheme of low and high-frequency coefficients based on four different fusion rules, namely maximum selection, maximum rule, gradient rule, and absolute maximum selection rule is presented. A series of experiments were conducted to evaluate the performance of the fusion, and the results showed that the proposed methods are superior to many of the current fusion methods.

ACKNOWLEDGMENT

Adnan H. Al-Hilali, Jamal S. Zraqou, Wessam Alkhadour, and Abdalla S. Al-Nuemi are grateful to Isra University, Amman, Jordan for the financial support granted to cover the publication fee of this research article.

REFERENCES

- [1] Pajares G., J. M. D. L. Cruz (2004). A wavelet-based image fusion tutorial. *Pattern Recognition*. Vol. 37, PP 1855–1872.
- [2] Aslantas V., R. Kurban (2010). Fusion of multi-focus images using differential evolution algorithm. *Expert Systems with Applications*; vol. 37, PP 8861–8870.
- [3] Duan J.Y., Meng G.F., Xiang S.M., Pan C.H. (2014). Multi focus image fusion via focus segmentation and region reconstruction. *NEUROCOMPUTING*, 140 (22), 193-209.
- [4] Jiang Q., Xin Jin, Shin-Jye Lee, Shaowen Yao (2017). A Novel Multi-Focus Image-fusion Method Based on Stationary.
- [5] Anjali Malviya, S.G. Bhirud (2009). Image-fusion of Digital Images, *International Journal of Recent Trends in*
- [6] H. Wang, J. Peng, W. Wu, Fusion algorithm for multisensor images based on discrete multiwavelet transform, *IEEE Proceedings of Vision, Image, and Signal Processing* 149(5), pp. 283–289 (2002).
- [7] S. Li and Y. Wang, Multisensor image fusion using discrete multiwavelet transform, in: *Proceedings of the 3rd International Conference on Visual Computing*, pp. 93–103 (2000). *Engineering*, Vol.2, No.3, PP 146-148.
- [8] Fann G. (2004). Singular operators in multiwavelet bases. *IBM J. res. & dev.* Vol. 48, No. 2.

- [9] Saleh Z. J. (2004). Video Image Compression based on Multiwavelets Transform. A thesis was submitted to the University of Baghdad, Iraq.
- [10] Geronimo J., D. Hardin, and P. R. Massopust (1994). Fractal Function and Wavelet Expansions Based on Several Functions. *Journal of Approximation Theory*, Vol.78, PP 373-401.
- [11] Martin M. B. (1999). Applications of Multiwavelets to Image Compression. Thesis in Electrical Engineering, Virginia Polytechnic Institute and State University (Virginia Tech), Blacksburg, Virginia.
- [12] Myna A. N., J. Prakash (2017). A Novel Hybrid Approach for Multi-focus Image-fusion using Fuzzy Logic and Wavelets. *International Journal of Emerging Trends & Technology in Computer Science (IJETTCS)*, Vol. 3, Issue 2.
- [13] Yu Liu, Lei Wang, Juan Cheng, Chang Li, Xun Chen (2020), Multi-focus image fusion: A Survey of the state of the art, *Information Fusion*, Volume 64, December 2020, Pages 71-91.